General Disclaimer

One or more of the Following Statements may affect this Document

- This document has been reproduced from the best copy furnished by the organizational source. It is being released in the interest of making available as much information as possible.

- This document may contain data, which exceeds the sheet parameters. It was furnished in this condition by the organizational source and is the best copy available.

- This document may contain tone-on-tone or color graphs, charts and/or pictures, which have been reproduced in black and white.

- This document is paginated as submitted by the original source.

- Portions of this document are not fully legible due to the historical nature of some of the material. However, it is the best reproduction available from the original submission.

NASA Technical Memorandum 78781

GEOMETRY REQUIREMENTS FOR UNSTEADY AERODYNAMICS IN AEROELASTIC ANALYSIS AND DESIGN

E. Carson Yates, Jr.
and
Luigi Morino

September 1978

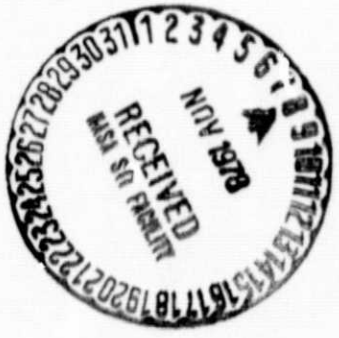

National Aeronautics and
Space Administration

Langley Research Center
Hampton, Virginia 23665

GEOMETRY REQUIREMENTS FOR UNSTEADY AERODYNAMICS IN AEROELASTIC ANALYSIS AND DESIGN

E. Carson Yates, Jr. and Luigi Morino

INTRODUCTION

Accurate calculation of aeroelastic characteristics required for the analysis and design of high-performance aircraft requires accurate and efficient evaluation of steady and unsteady aerodynamic loads on aircraft having arbitrary shapes and motions, including structural deformations. This presentation will address the aircraft geometry requirements for unsteady aerodynamic computations and will emphasize differences between requirements for steady and unsteady flow.

COMPARISON OF STEADY AND UNSTEADY FLOW REQUIREMENTS

(Figure 1)

Requirements for aeroelastic analysis and design are in several respects more complicated and more severe than for the more conventional steady-state aerodynamics. For example: (1) The aeroelastician deals with flexible structures so that even in steady-state conditions, the aerodynamic load is a function of structural deformation, and vice versa. (2) The unsteady aerodynamic formulations required in dynamic aeroelasticity involve complex quantities (e.g., normalwash velocities, aerodynamic influence functions, and pressure) that manifest time- or frequency-dependent attenuations and phase shifts relative to steady state. (3) In dynamic aeroelasticity--flutter, for example--the aeroelastician must evaluate pressure distributions for vibration mode shapes that are much more wiggly than a typical steady-state mean-camber surface. The corresponding pressure distributions will also be more wiggly than those for steady state so that computational convergence requirements are usually more severe than for steady state. (4) Flutter analyses, as well as iterative structural resizing, require evaluation of pressure distributions for a multiplicity of mode shapes, frequencies, aircraft loading conditions, etc. Consequently, computational efficiency is vital, and it is essential to minimize the amount of recomputation required when mode shapes and/or frequencies are changed.

With these thoughts in mind, we shall discuss geometry requirements within the framework of the SOUSSA aerodynamic formulation because it is the most general potential-flow program that we now have under development (with regard to aircraft geometry, motion and deformations, and speed ranges) and because present and future SOUSSA geometry requirements are as stringent as those for any aerodynamic program that we now anticipate. Geometry required is considered to be composed of three parts: (1) shape of vehicle, (2) orientation of vehicle, (3) deformation(s). Orientation involves little more than a rotation of coordinate axes and consequently will not be emphasized here. Deformations can be finite but are more usually taken to be infinitesimal and approximated by a linear combination of the natural undamped vibration modes of the aircraft. As many as two dozen modes or more may be required to converge the aeroelastic solution. A related geometrical requirement is determination of wake shape which is not known a priori although it may be assumed to be flat for many applications.

STEADY, OSCILLATORY AND UNSTEADY SUBSONIC AND SUPERSONIC AERODYNAMICS

(SOUSSA)

Objective: An accurate, general, unified method for calculating steady and unsteady loads on complete aircraft with arbitrary shape and motion in subsonic or supersonic flow, with emphasis on application in computer-aided structural design

Approach: Green's theorem is used to formulate exact integral equation for potential.

$$\varphi(P,t) = \iiint\!\!\iint G F \, dV_1 dt_1 + \iiint \left[\nabla_1 S \left(G\nabla_1\varphi - \varphi\nabla_1 G\right) - \frac{1}{a^2}\frac{dS}{dt_1}\left(G\frac{d\varphi}{dt_1} - \varphi\frac{dG}{dt_1}\right)\right] |\Box S|^{-1} \, dS \, dt_1$$

where φ = perturbation velocity potential
G = Green's function
F = nonlinear terms
$S(x, y, z, t) = 0$ defines body surface

$$|\Box S| = \sqrt{S_x^2 + S_y^2 + S_z^2 + S_t^2}$$

$$\frac{d}{dt_1} = \frac{\partial}{\partial t_1} + U_\infty \frac{\partial}{\partial x_1}$$

Exact boundary condition on body is

$$\frac{DS}{Dt} = \frac{\partial S}{\partial t} + \nabla\Phi \cdot \nabla S = \frac{\partial S}{\partial t} + U_\infty (\vec{i} + \nabla\varphi) \cdot \nabla S = 0$$

Figure 2

STEADY, OSCILLATORY AND UNSTEADY SUBSONIC AND SUPERSONIC AERODYNAMICS

(SOUSSA)

(Figure 2)

To set the stage, a brief review of SOUSSA formulation is in order. Application of Green's theorem leads to an integral equation for the perturbation velocity potential ϕ at any point P in the flow or on the flow boundary (i.e., on S). Note that the second integral contains only linear terms which are integrated over the boundary surface S, whereas the first integral contains nonlinear terms F, involving products of derivatives of ϕ, which must be integrated over the fluid volume.

The boundary condition clearly shows the effect of time variation of S. If the variation is harmonic, for example, the $\frac{\partial S}{\partial t}$ term becomes $i\omega S$ so that the normalwash at $S = 0$ becomes complex. The imaginary part, however, involves only surface ordinates (including displacements and deformations), whereas the real (steady-state) part involves derivatives of surface ordinates. Thus, introduction of unsteadiness does not impose more stringent requirements on surface definition as far as quantities required are concerned. It may, however, require greater accuracy and greater amounts of geometrical information (e.g., for more points on the surface) in order to define adequately the wiggly modes of deformation referred to previously.

The influence of nonlinear terms F is being studied in the development of SOUSSA aerodynamics for the transonic range. However, these terms are not included in the present computer program.

SOLUTION OF INTEGRAL EQUATION

Solution by spatial discretization with arbitrary nonplanar quadrilateral surface panels and time solution by Laplace transform results in

$$[\tilde{Y}_{jh}]\{\tilde{\Phi}_h\} = [\tilde{Z}_{jh}]\{\tilde{\Psi}_h\}$$

where $\tilde{\Phi}_h$ = Laplace transform of perturbation velocity potential
$\tilde{\Psi}_h$ = Laplace transform of normalwash

$$\tilde{Y}_{jh} = \delta_{jh} - (C_{jh} + s D_{jh}) e^{-s\theta_{jh}} - \sum_n (F_{jn} + s G_{jn}) S_{nh} e^{-s(\theta_{jn} + \Pi_n)}$$

$$\tilde{Z}_{jh} = B_{jh} e^{-s\theta_{jh}}$$

s = Laplace transform variable

B_{jh}, C_{jh}, D_{jh}, F_{jn}, G_{jn} = integrals over surface panels, independent of normalwash and s

θ_{jh}, Π_{jh} = lag functions

$S_{nh} = \pm 1$

Surface pressures are obtained from Bernoulli's equation.

Figure 3

SOLUTION OF INTEGRAL EQUATION

(Figure 3)

Assuming that the effect of the motion of the surface is negligible except in the boundary condition (infinitesimal unsteady deformation) and neglecting the nonlinear terms, then surface paneling and Laplace transform solution yield a matrix equation relating the unknown potential ϕ on the vehicle surface to the normal wash ψ. Elements of the coefficient matrices are independent of normalwash (and hence deformation) and are simple functions of the Laplace variable s. For a given paneling arrangement, they depend only on Mach number.

Use of arbitrary nonplanar quadrilateral panels permits matching nodes of the aerodynamic panels to the nodes of a structural finite-element model, if desired, in order to use the nodal coordinates and calculated displacements directly without requirement for interpolation. In general, however, solution for the velocity-potential matrix requires the following geometrical input: (1) Coordinates of panel nodes usually obtained by interpolation (lofting) from aircraft shape information. (2) Time-dependent normalwash at control points which usually do not coincide with panel nodes. Normalwash involves coordinates and slopes obtained from aircraft shape plus orientation plus deformation.
Note that increasing the number of deformation modes used involves only adding columns to the ψ and ϕ matrices, and that updating the entire set of deformation modes, as in a structural design application, involves only replacing the ψ matrix. The Y and Z matrices are unaffected in either case.

Surface pressures are obtained from Bernoulli's equation. Generalized aerodynamic forces, including aerodynamic coefficients and stability derivatives, are determined from weighted integrals of the pressure which require values of surface displacement (due to rigid-body rotation and/or modal deformation) at a set of integration points which may not coincide with the panel nodes nor control points.

The geometrical information required by SOUSSA can, of course, be generated with any suitable geometry preprocessor as long as the results are cast in required SOUSSA input format. It is evident, however, that automatic paneling capability is essential to the efficient processing of complicated shapes and deformations that may require many hundreds of panels. Such capability should include not only automatic calculation of the coordinates of nodes, control points, and integration points, but also automatic identification numbering for these points as well as for the panels and systematic identification of which nodes go with which panels.

GENERAL POTENTIAL-FLOW AERODYNAMICS

(SOUSSA)

GENERAL FINITE-ELEMENT METHOD:

- ARBITRARY COMPLETE A/C CONFIGURATION
- STEADY AND GENERAL UNSTEADY MOTION
- SUBSONIC AND SUPERSONIC
- COMPUTATIONAL EFFICIENCY

CURRENT DEVELOPMENTS:

- NONLINEAR EFFECTS (TRANSONIC FLOW, WAKE DEFORMATION)
- IMPROVED FINITE ELEMENTS (HIGHER ORDER, SPECIAL PURPOSE)
- ROTATIONAL FLOW (TURBULENCE, VISCOSITY)

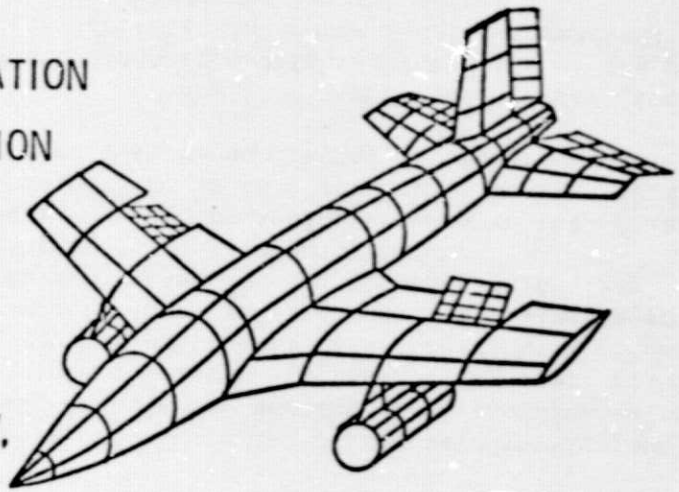

Figure 4

GENERAL POTENTIAL-FLOW AERODYNAMICS

(SOUSSA)

(Figure 4)

The upper part of this figure lists some of the fea ures of the SOUSSA aerodynamic formulation. The lower part indicates some expanded capabilities and imprcvements that are under development and that will influence surface geometry requirements. These are discussed in the following figures.

SURFACE OF INTEGRATION S

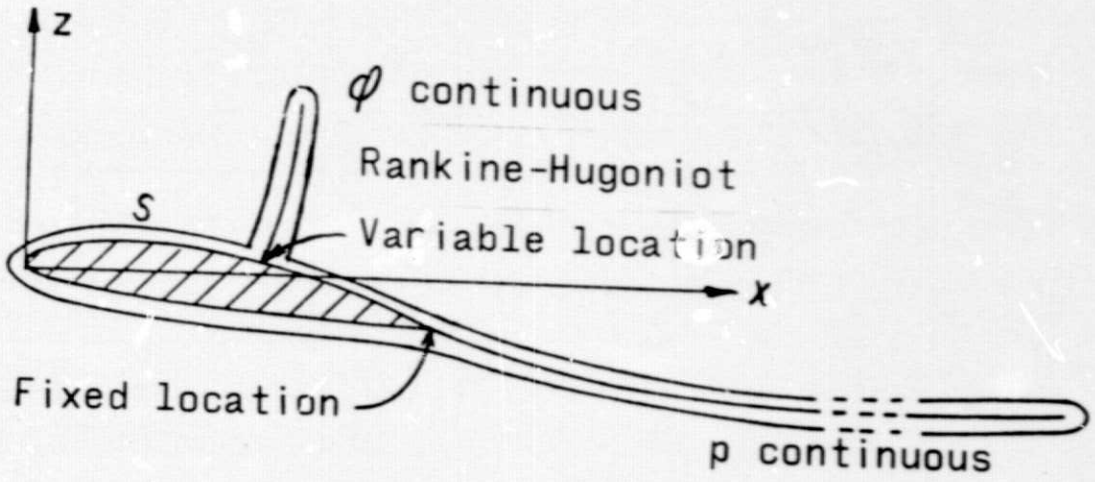

Figure 5

SURFACE OF INTEGRATION S

(Figure 5)

In the integral equation for the velocity potential (previously shown) the surface integration extends over the surface of the aircraft plus its wake, and the no-penetration boundary condition DS/Dt = 0 applies over both. Moreover, the pressure must be continuous across the wake although the potential is discontinuous. The forward edge of the wake of a lifting surface is considered to be located at the lifting-surface trailing edge, but the position of the rest of the wake is not known a priori, is variable, time-dependent, and must be determined in the calculation. This variability requires relocation and reorientation of the wake and its panels during the calculation, perhaps many times if the calculation is iterative.

This figure also shows a shockwave which is isolated from the flow field by a portion of the surface S. Over this portion of S the no-penetration boundary condition must be replaced by Rankine-Hugoniot conditions or other shock conditions which quantify shock-induced discontinuities in derivatives of the potential although the potential itself is continuous across the shock. These discontinuities make it desirable to have panel edges lie along the foot of the shock. But shock location, shape, extent, strength, and velocity relative to the vehicle surface are time dependent. Moreover, motion of finite amplitude--even small amplitude--that is needed to investigate limit-cycle aeroelastic response can lead to large-amplitude shock motion and even discontinuous shock location. Consequently, requiring panel edges to coincide with the foot of the shock can require extensive repaneling in the vicinity of the shock during calculations for unsteady motion. In contrast, nonlinear calculations for shock-free transonic flow require no repaneling and impose no special requirements for surface geometry.

WAKE-FUSELAGE INTERSECTION

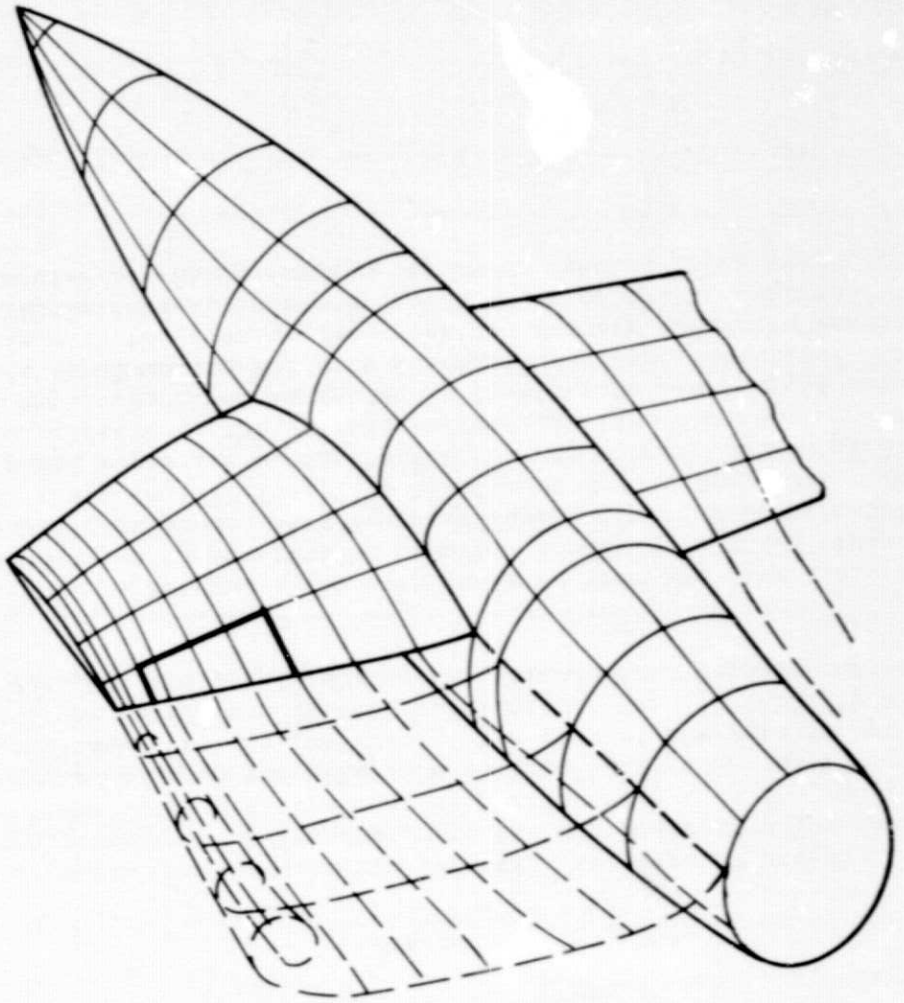

Figure 6

WAKE-FUSELAGE INTERSECTION

(figure 6)

Shocks and wakes from lifting surfaces impinge upon fuselages or other portions of the vehicle along lines that are time dependent. Because of the discontinuities in potential or its derivatives at these impingement lines, it is desirable that panel edges coincide with them. Hence, time dependent repaneling in these vicinities is also indicated.

For simplicity in its development, the present SOUSSA program contains zeroth-order (constant-potential) aerodynamic elements. However, it has been intended from the beginning that the program would employ higher-order elements in order to reduce the number of elements required to converge the solution. Such elements have been developed and will soon be incorporated into the program. In addition, special-purpose elements are being developed for paneling in regions where correct variation of potential is theoretically known. These elements have built-in shape functions to produce the correct variation of potential, for example, adjacent to normalwash discontinuities such as control-surface hinge lines and side edges, or correct variation of potential derivatives as at subsonic trailing edges. In addition, flow-through elements are required to model engine thrust in nacelles and to panel shockwaves. Such elements impose no new requirements for surface geometry information. Note that no special panels are required adjacent to shock or wake impingement on the body surface. Use of higher-order and special-purpose elements should reduce computer time and storage requirements but probably will do little to reduce the amount of geometrical input information required. Although fewer elements are used, more information is required per element. Detailed accuracy of information out requires detailed accuracy of information in, irrespective of the level of sophistication.

Finally, incorporating the effects of viscosity and rotational flow will impose a requirement for relatively high accuracy of computed pressure gradients and hence will require higher-order elements (at least third order) than would be required for most potential-flow problems. Alternatively, it is possible that required accuracy and order of continuity may be attained from solutions using lower-order elements followed by spline (or other) interpolation of the calculated potential.

Specific treatment of aircraft geometry in the SOUSSA program itself will next be described.

POTENTIAL-NORMALWASH RELATIONSHIP

$$\boxed{\underline{\tilde{\varphi}} = \underline{\tilde{E}}_2\ \underline{\tilde{\psi}}} \qquad (\underline{\tilde{E}}_2 = \underline{\tilde{Y}}^{-1}\ \underline{\tilde{Z}}) \qquad (1)$$

WITH

$$\tilde{Y}_{jh} = \delta_{jh} - (C_{jh} + s D_{jh})\, e^{-s\Theta_{jh}} + \sum_n (F_{jn} + s G_{jn})\, S_{nh}\, e^{-s(\Theta_{jn}+\Pi_n)}$$

$$\tilde{Z}_{jh} = B_{jh}\, e^{-s\Theta_{jh}}$$

WHERE, FOR INSTANCE,

$$B_{jh} = \frac{1}{2\pi} \iint_{\sigma_h} \frac{1}{R}\, d\sigma_h \Big|_{P=P_j} \qquad C_{jh} = \frac{1}{2\pi} \iint_{\sigma_h} \frac{\partial}{\partial N}\frac{1}{R}\, d\sigma_h \Big|_{P=P_j}$$

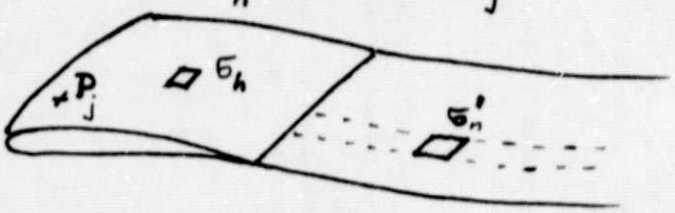

HYPERBOLOIDAL ELEMENT

BOUNDARY CONDITIONS

GIVEN $\vec{v} = -U_\infty \vec{i} + \sum_m \dot{q}_m \vec{M}_m$ AND $\vec{n} = \vec{n}_s + \sum_m q_m \Delta\vec{n}_m$

$\psi \equiv \dfrac{\partial\phi}{\partial N} = \vec{v}\cdot\vec{n}$ YIELDS $\boxed{\underline{\tilde{\psi}} = \underline{\tilde{E}}_1\ \underline{\tilde{\dot{q}}}}$ (2)

BERNOULLI'S THEOREM

$$C_p = -2\left(\frac{\partial\varphi}{\partial t} + U_\infty \frac{\partial\varphi}{\partial x}\right) \quad \text{YIELDS} \quad \boxed{\underline{\tilde{C}}_p = \underline{\tilde{E}}_3\ \underline{\tilde{\varphi}}} \qquad (3)$$

GENERALIZED FORCES

$$e_m = \oiint (-C_p \vec{n}\cdot\vec{M}_m)\, d\Sigma \quad \text{YIELDS} \quad \boxed{\underline{\tilde{e}} = \underline{\tilde{E}}_4\ \underline{\tilde{C}}_p} \qquad (4)$$

COMBINING

$$\boxed{\underline{\tilde{e}} = \underline{\tilde{E}}\ \underline{\tilde{\dot{q}}}} \qquad (\underline{\tilde{E}} = \underline{\tilde{E}}_4\ \underline{\tilde{E}}_3\ \underline{\tilde{E}}_2\ \underline{\tilde{E}}_1) \qquad (5)$$

Figure 7

POTENTIAL-NORMALWASH RELATIONSHIP

(Figure 7)

The rest of this presentation is devoted to the specific geometry requirements for the program SOUSSA P (Steady, Oscillatory and Unsteady, Subsonic and Supersonic Aerodynamics; Production Version). As presented above, the Green's function method yields an integral equation over the surface of the aircraft and its wake (with differential-delay dependence on time). Dividing the surfaces in quadrilateral elements and assuming the potential, the normalwash and the potential discontinuity to be constant within each element, one obtains Eq. (1).

The coefficients B_{jh}, C_{jh}, etc., are evaluated analytically, with the original surface σ_h approximated by a hyperboloidal paraboloid (hyperboloidal element). Low-order numerical quadrature is used for distant elements.

In order to complete the formulation three additional relationships are required:

1. Boundary conditions, relating normalwash ψ to the generalized coordinates q_m (Eq. 2)
2. Bernoulli's theorem relating pressure coefficient C_p to potential ϕ (Eq. 3)
3. Definition of generalized forces, e_m, as functionals of the pressure coefficient C_p (Eq. 4)

Finally combining Eqs. 1 to 4 one obtains the matrix $\tilde{E}$ relating the generalized forces, e_m, to the generalized coordinates, q_m.

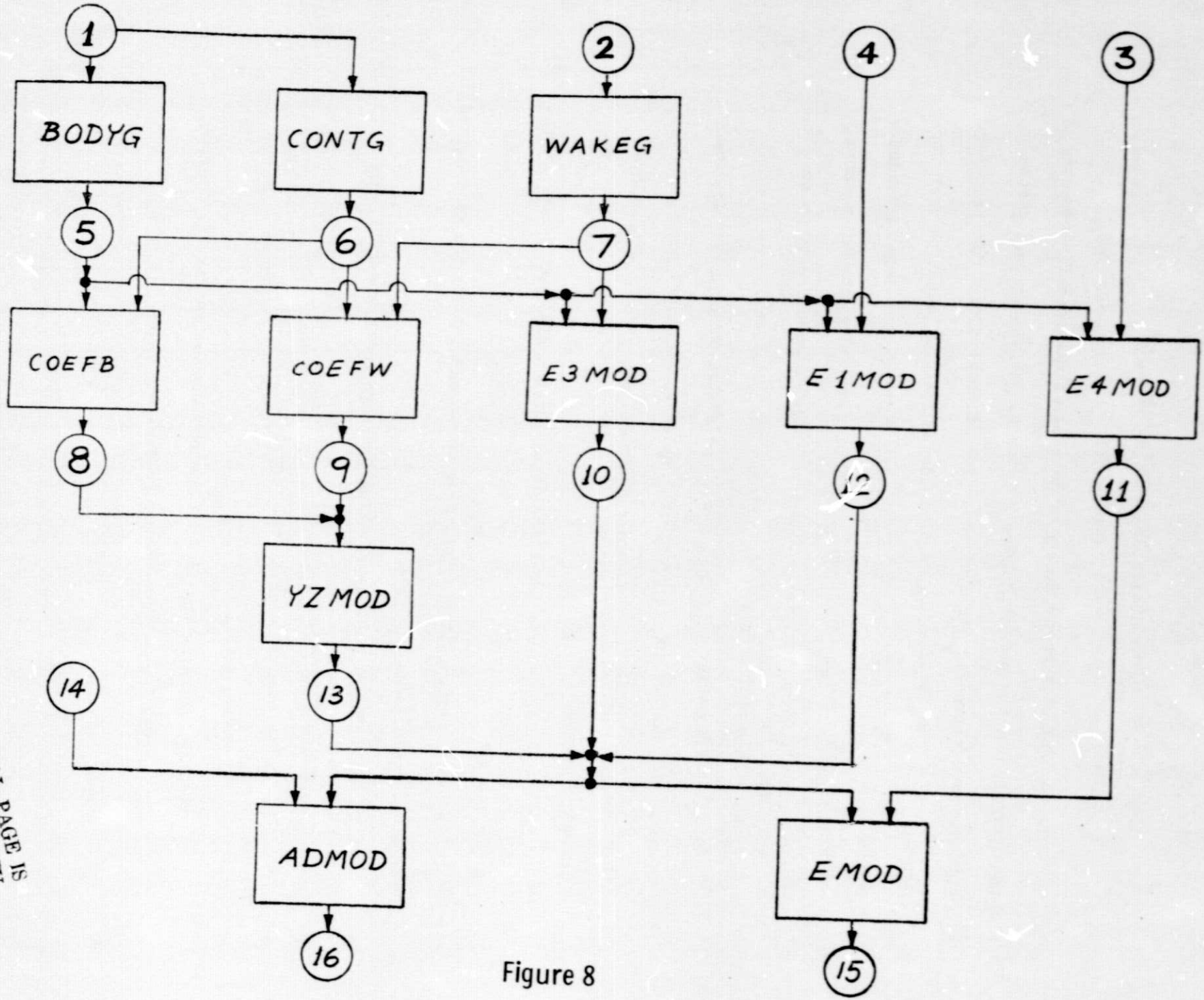

Figure 8

SOUSSA P 1.1

(Figure 8)

This figure shows the flow chart for the program SOUSSA, and it is presented in order to indicate how the geometric information is used in the program. The check points will be discussed later. Here only the function of each module is briefly described.

Interfaces

BODYG, CONTG and WAKEG: Elaborate the geometry input of checkpoints 1 and 2 (user oriented) into the checkpoints 5, 6 and 7 as needed in the rest of the program.

Potential-Normal wash relationship (mode independent)

COEFB: evaluates the body coefficients B_{jh}, C_{jh}, D_{jh} and ∂_{jh}

COEFW: evaluates the wake coefficients F_{jn}, G_{jn}, S_{nh}, Θ_{jn} and π_n

YZMOD: combines the above frequency-independent coefficients to yield the frequency-dependent matrices $[Y_{jh}]$ and $[Z_{jh}]$

Boundary conditions (mode dependent)

E1MOD: evaluates the matrix $\underline{\tilde{E}}_1$ relating $\underline{\tilde{\psi}}$ to $\underline{\tilde{q}}$

Bernoulli's Theorem (mode independent)

E3MOD: evaluates the matrix $\underline{\tilde{E}}_3$ relating $\underline{\tilde{C}}_p$ to $\underline{\tilde{\phi}}$

Generalized Forces (mode dependent)

E4MOD: evaluates the matrix $\underline{\tilde{E}}_4$ relating $\underline{\tilde{e}}$ to $\underline{\tilde{C}}_p$

Combining

EMOD: evaluates the generalized-aerodynamic-force matrix

$$\underline{\tilde{E}} = \underline{\tilde{E}}_4 \underline{\tilde{E}}_3 \underline{\tilde{E}}_2 \underline{\tilde{E}}_1$$

ADMOD: implements an aerodynamic design method which yields the shape from a prescribed pressure distribution.

CHECKPOINT #1

- Cartesian coordinates of nodes, $\vec{P}_n$.
- $i_n\,(i_E, i_K)$: matrix relating node number to element and corner numbers.
- body-symmetry code numbers.
- code number for elements (e.g. TE, hinge, ..)

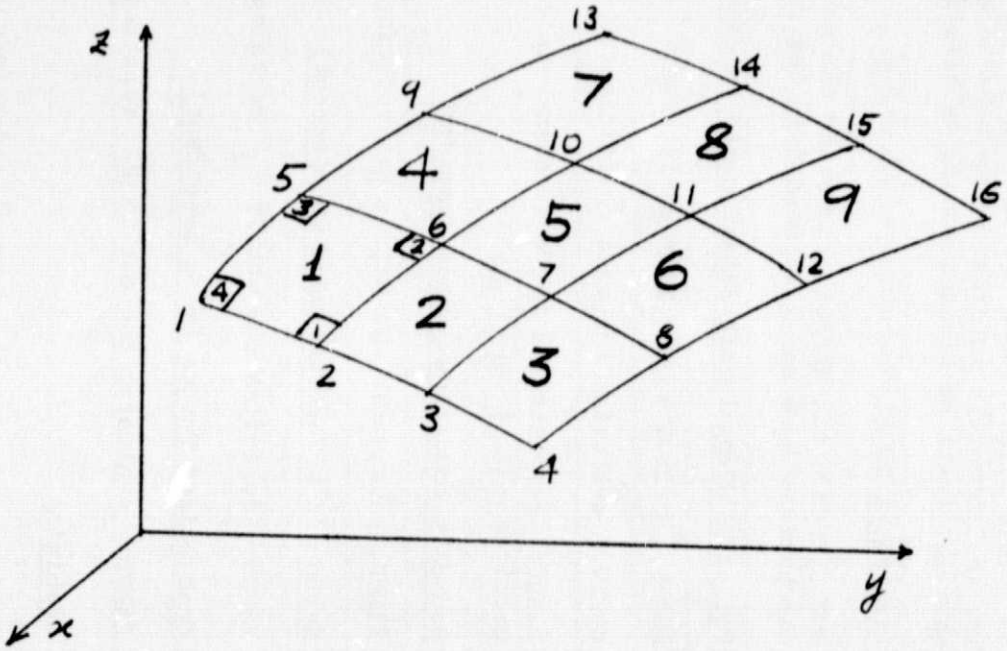

Figure 9

CHECKPOINT #1

(Figure 9)

This figure presents the contents of Checkpoint #1 (input to module BODYG), which consists of information describing the geometry of the aircraft body. It is user-oriented in that the quantities required are compatible with the output of state-of-the-art geometry preprocessors. Also, if the aircraft is symmetric with respect to the x-z plane, then only the right half need be supplied. The same is true for the x-y plane.

Regarding the individual components of Checkpoint #1:

- The Cartesian coordinates of the nodes are assumed to be those of the aircraft already oriented as desired by the user.
- Referring to the example depicted in the figure, element number 1, corner 1 yields node number 2.
- The body-symmetry code numbers reflect whether symmetry is considered with respect to the x-z and/or y-z planes.
- The element code numbers provide information such as whether or not a wake emanates from an edge of an element, or if an edge coincides with a hinge line, etc.

CHECKPOINT # 2

- Cartesian coordinates of corners of wake strips
- Symmetry codes for each strip
- Matrix relating each strip to the four corresponding trailing edge elements.
- Number of element per strip.

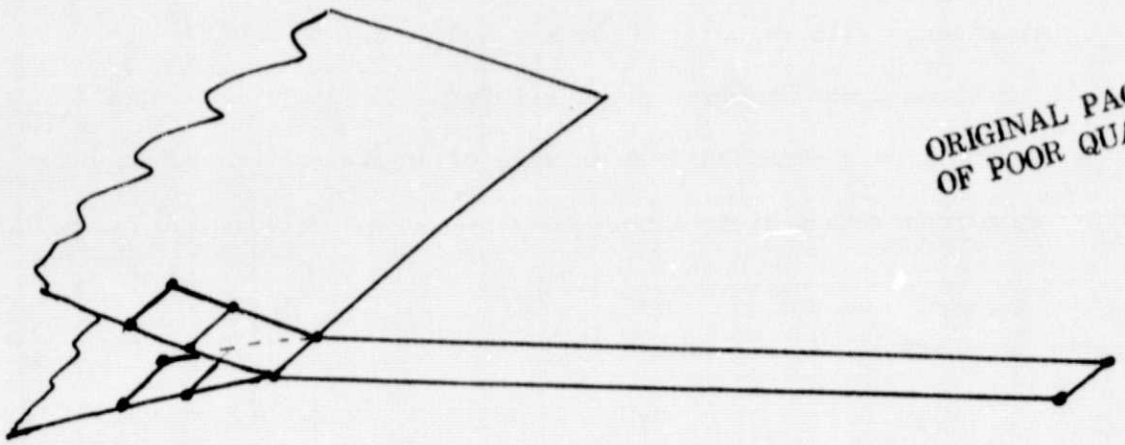

CHECKPOINTS # 3 AND 4

3-D (vector) mode shapes, $\vec{M}_m(P_h)$, at nodes, P_h

Figure 10

CHECKPOINTS #2, 3 AND 4

(Figure 10)

This figure presents the contents of Checkpoints #2 (input to Module WAKEG), #3 (input to Module E4MOD) and #4 (input to Module E1MOD).

Checkpoint #2 consists of information describing the geometry of the wake. By describing the wake as a collection of strips, many different forms of input can easily be made compatible. If a wake strip is symmetric with respect to the x-z plane, then only the right half need be supplied (same for the x-y plane).

Also,

- o Desired orientation of the wake with respect to the aircraft is assumed to already be satisfied.
- o The matrix which relates each wake-strip number with the corresponding four trailing-edge element numbers is used in evaluating the trailing edge values of the potential and for determining the values of the pressure discontinuity at the centroid of the trailing-edge elements.

Checkpoint #3 corresponds to the generalized-forces deformation modes, and Checkpoint #4 corresponds to the boundary-condition deformation modes.

CHECKPOINT #5

- Same quantities as checkpoint #1, but for complete aircraft
- base vectors $\vec{a}_1$ and $\vec{a}_2$ and normal $\vec{a}_1 \times \vec{a}_2$ at centroids of elements for complete aircraft

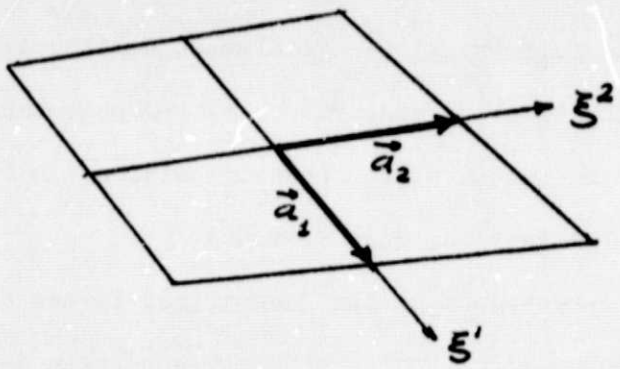

CHECKPOINT #6

- Cartesian coordinates of the centroids of the elements

Figure 11

CHECKPOINTS #5 AND 6

(Figure 11)

This figure presents the contents of Checkpoints #5 (input to module COEFB) and #6 (input to modules COEFB and COEFW). These checkpoints are at a lower level than checkpoints #1-4 if one views the SOUSSA P flow diagram as a top-down representation. The implications of this are that these checkpoints are not as "user-oriented" as higher-level checkpoints, since program execution has progressed to this point. This is evidenced by the fact that for Checkpoint #5, the same quantities as Checkpoint #1 are required except that symmetry conditions (and their advantages in preparing geometrical input) are not considered. Furthermore, geometrical quantities such as the base vectors and normals of surface elements are not as readily available from geometry preprocessors as the information contained in Checkpoint #1. These considerations must be accounted for by those users desiring to begin execution of SOUSSA P at this level.

For version 1.1 of SOUSSA P, the location of the control points must be specified as the geometrical centroids of the body elements. For future versions (first-order finite element formulation), the location of the nodes will be the necessary input.

CHECKPOINT #7

- Cartesian coordinates of the corners of the wake elements for the entire wake.
- Matrix relating each wake element to the four trailing-edge elements (see checkpoint # 2), for the entire wake.
- Matrix relating each wake element to the coefficients of influence, ±1, for the two trailing edge elements

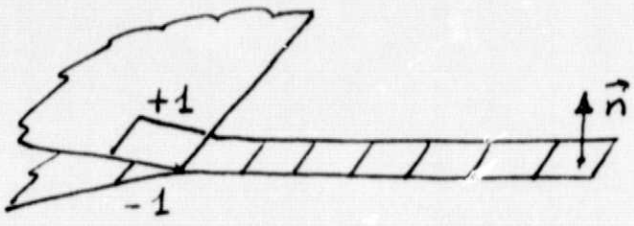

Figure 12

CHECKPOINT #7

(Figure 12)

This figure presents the contents of Checkpoint #7 (input to module COEFW). This is also not a top-level checkpoint, hence, its contents may not be as "user-oriented" as, say, Checkpoint #2. For instance, at this level:

- The coordinates of the wake elements (as opposed to the wake strips) are required, and no symmetry conditions may be taken advantage of (i.e., all the elements must be input).
- The matrix used in correction for the trailing-edge potential values, for example, must be given for the elements comprising the complete wake.
- Most geometry preprocessors would not provide the matrix of the coefficients of influence of the trailing-edge elements that determines the value of the potential discontinuity for each wake element. Note for SOUSSA P 1.1 these coefficients are simply 1 and -1, but for later versions, splines could be used to determine these coefficients.

FIRST-ORDER FINITE ELEMENT (UNDER DEVELOPMENT)

- SIMILAR FLOW CHART
- ALMOST IDENTICAL INPUT (CHECKPOINTS 1 TO 4)

TRANSONIC UNSTEADY FLOW (UNDER CONSIDERATION)

$$2\pi\phi = -\oint\!\!\oint_{\text{AIRCRAFT}} \left(\psi^{\theta} \frac{1}{R} - \phi^{\theta} \frac{\partial}{\partial N} \frac{1}{R} + \dot{\phi}^{\theta} \frac{1}{R} \frac{\partial R}{\partial N} \right) d\Sigma_A$$

$$+ \iint_{\text{WAKE}} \left(\Delta\phi^{\theta} \frac{\partial}{\partial N} \frac{1}{R} - \Delta\dot{\phi} \frac{1}{R} \frac{\partial R}{\partial N} \right) d\Sigma_W$$

$$+ \iiint_{\text{VOLUME}} \left(\phi_x \phi_{xx} \right)^{\theta} \frac{1}{R} \, dV - \iint_{\text{SHOCK}} \Delta\psi^{\theta} \frac{1}{R} \, d\Sigma_S^{\theta}$$

(NEW TERMS)

- REQUIRES FINITE ELEMENTS IN REGION SURROUNDING AIRCRAFT

Figure 13

CURRENT DEVELOPMENTS

(Figure 13)

Work now under consideration includes higher-order finite-element formulations. In particular, work on first-order finite element is now underway. Splines are also being considered for various modules.

Also under consideration is the extension to transonic unsteady flow. This requires the addition of two terms, the first is due to the non-linearities in the differential equation, the second to the presence of shocks. The equation is solved step-by-step in the time domain. The location of the shock and its intensity are obtained at each time step.